Master's Thesis of Science

# The irradiation effect on malignant phyllodes tumor (MPT) of the breast in patient-derived xenograft model and its derived cells

환자 유래 이종이식 모델(patient-derived xenograft model) 및 세포를 이용한 유방 악성엽상종양의 방사선 치료 효과에 관한 연구

August 2023

Graduate School
Seoul National University College of Medicine
Interdisciplinary Program in Cancer Biology

Haritonova Valentina

# The irradiation effect on malignant phyllodes tumor (MPT) of the breast in patient-derived xenograft model and its derived cells

Examined by Hong-Kyu Kim

Submitting a master's thesis of
Science

April 2023

Graduate School
Seoul National University College of Medicine
Interdisciplinary Programs in Cancer Biology

Haritonova Valentina

Confirming the master's thesis written by
Haritonova Valentina
July 2023

| | | |
|---|---|---|
| Chair | Wonshik Han | (Seal) |
| Vice Chair | Hyeong-Gon Moon | (Seal) |
| Examiner | Hong-Kyu Kim | (Seal) |

# Abstract

The current therapeutic strategy for managing malignant phyllodes tumors (MPTs) is wide excision. However, despite achieving negative surgical margins, this approach is associated with a certain rate of local recurrence. As a potential therapeutic strategy for high-risk patients, radiotherapy is considered, but its efficacy is still debatable. In our study, we demonstrated the positive impact of radiation treatment in in vivo PDX mouse models, where significant tumor growth suppression and decreased mitotic count were observed in the irradiated group compared to the control. Our histological evaluation also indicated a reduced tendency for stromal cellularity and pleomorphism in the irradiated group. Analysis of differentially expressed genes (DEGs) after tumor resection revealed upregulation of the p53 signaling pathway and I-kappa B kinase/NF-kappa B signaling pathway. Two genes with high fold-change values, MDM2 and DDB2, associated with these pathways, were significantly upregulated in the irradiated group. We found that the radiation-induced upregulation of DDB2 and MDM2 was conserved in Phyllodes tumor cells and tumor models, but not in Breast Cancer cells. Additionally, cells deficient in DDB2 and MDM2 demonstrated a decreased proliferation rate. While DDB2 deficiency tends to promote S/G2M cell cycle transition, overall apoptosis overrode this effect. MDM2 deficiency did not significantly alter apoptosis or cell cycle distribution in PDX78 cells. Radiation treatment (24Gy) eliminated the difference in pre-existing proliferation rate in PDX78 cells, suggesting a potential role for other upregulated genes or pathway interactions in response to radiation. Furthermore, deficiency in DDB2 and MDM2 in PDX78 cells led to an increase in cell migration and invasion, suggesting diverse roles for these genes in different cancer stages. Contrary to initial hypotheses, our research did not provide evidence to support the concept that upregulation of DDB2 and MDM2 contributes to radioresistance in Phyllodes tumor cells.

However, we posit that an upregulation of these genes might play a role in diminishing the proliferation of Phyllodes tumor cells under the effect of radiotherapy. Furthermore, this could potentially result in a reduction of cell migration and invasion capacities, potentially inhibiting metastasis.

**Keywords:** Phyllodes tumor, Radiation therapy, PDX model, DDB2, MDM2
**Student Number:** 2021-22873

The author of this thesis is a Global Korea Scholarship scholar sponsored by the Korean Government

# Table of Contents

# List of Tables

# List of Figures

# List of Abbreviations

BC – Breast Cancer
CTL – Control
DDB2 – Damage specific DNA binding protein 2
DEGs – Differentially Expressed Genes
DFS – Disease Free Survival
DMSO – Dimethyl sulfoxide
FACS – Fluorescence-activated cell sorting analysis
FC – Fold change
GTG – G-bands by Trypsin using Giemsa staining technique
HBP1 – HMG-Box Transcription Factor 1
HDAC1 – Histone deacetylase 1
HER2 – Human epidermal growth factor receptor 2
HNSCC – Oral/Head and Neck Squamous Cell Carcinoma
HPF – High-power field
HR – Homologous Recombination
IkBa – Nuclear factor kappa B inhibitor alpha
KEGG pathway – Kyoto Encyclopedia of Genes and Genomes
LR – Local Recurrence
MDM2 – MDM2 proto-oncogene (murine double minute 2)
MMP9 – Matrix metallopeptidase 9
MnSOD – Mitochondrial superoxide dismutase 2
NER – Nucleotide Excision Repair
NFkB – Nuclear Factor kappa B
ns – Not significant
NSCLC – non-small cell lung cancer
OS – Overall Survival
qPCR – Quantitative Real-time polymerase chain reaction
PDX – Patient-derived xenograft
PFA – Paraformaldehyde
PIK3CA – Phosphatidylinositol-4,5-bisphosphate 3-kinase catalytic subunit alpha
PTs – Phyllodes Tumors

RARA – Retinoic acid receptor alpha

RT – Radiation Treatment

SBR grading – Scaff–Boom–Richardson grading

siRNA – Small interfering RNA

SD – Standard Deviation

SDS–PAGE – sodium dodecyl sulfate–polyacrylamide gel electrophoresis

TP53 – Tumor protein p53

UTR – Untranslated region

# Chapter 1. Introduction

Phyllodes tumors, a subset of breast tumors with a unique fibroepithelial origin and leaf-like appearance, account for 0.3 to 1% of all breast tumors [1-3]. These tumors are classified as high risk due to their considerable local recurrence rate of 21% within 2-3 years post-diagnosis. Distant metastasis, primarily to the lung and skeleton, is also seen in up to 28% of malignant Phyllodes tumors. Unlike many other breast tumors, axillary lymph node metastases are rare and surgical removal is typically not required [1,2,4,5].

Phyllodes tumors are categorized by the World Health Organization (WHO) as benign, borderline, or malignant, based on various histological, molecular, and other tumor characteristics. This diagnosis is comprehensive and includes considerations of factors such as morphological heterogeneity, epithelial-stromal ratio, stromal hypercellularity, nuclear atypia, mitotic count, stromal overgrowth, and tumor margin. These characteristics differ in severity from benign to malignant Phyllodes tumors. Despite these classifications, Phyllodes tumors pose a diagnostic challenge. They are hard to differentiate from fibroadenomas, especially in their benign state, and other metaplastic carcinomas, which share similar morphological and histological characteristics. An interdisciplinary approach is necessary for diagnosis, encompassing histological characteristics and additional molecular analyses, such as panels for cytokeratins, p63, and CD34, along with investigation of mutations in genes such as MED12, TP53, RARA, and PIK3CA [1,3].

Treatment strategy for Phyllodes tumors primarily involves wide surgical excision without axillary lymph node dissection. The application of adjuvant chemotherapy in the treatment of Phyllodes tumors is uncertain due to the lack of clear evidence from numerous studies linking its use to improved disease-free survival. Several reasons could contribute to this lack of clear correlation. However, for high-risk patients – particularly those presenting with

extensive stromal overgrowth or large tumors exceeding 5 cm in diameter – adjuvant chemotherapy could be considered as an optional treatment strategy [1].

The impact of radiation therapy remains contentious, with studies suggesting that it may reduce local recurrence rates but not affect disease-free survival or overall survival rates. The role of adjuvant chemotherapy is also uncertain, with many studies unable to demonstrate a correlation between chemotherapy and improved disease-free survival.

In this study, we aim to examine the effect of radiation treatment on Phyllodes tumors at both in vivo and in vitro levels using patient-derived xenograft (PDX) models and cells derived from them.

## 1.1. Study Background

First, we used Patient-Derived Xenograft (PDX) models to evaluate the impact of radiation treatment on malignant phyllodes tumors (MPTs). Human MPT tumor tissues were transplanted into the abdominal mammary glands of these models, with each graft measuring 1 $mm^3$ . Once the tumors in the PDX models reached a size of 400 $mm^3$ , we applied radiation in four fractions of 6 Gy (totaling 24 Gy) at 24-hour intervals. We carried out histological examinations and differential gene expression analyses on the tumors, which were resected either 15 days after irradiation or upon reaching a size of 1000 $mm^2$ .

Our preliminary findings revealed a significant suppression of tumor growth in the irradiated group compared to the control (n=3, P=0.015, Wilcoxon test) (Figure 1). Upon histological examination (Table 1), the irradiated group exhibited a lower mitotic count (mitoses/10 High Power Field (HPF), 2.3 ± 3.2 vs. 22.0 ± 11.1, p=0.04), and presented reduced tendencies towards stromal cellularity and pleomorphism (p=0.057, p=0.184, respectively). No differences were found concerning stromal overgrowth, and distant metastasis was not observed in either the irradiated or control

groups.

We identified 25 genes with upregulated values in the irradiated group compared to the control group (log2 fold change > 1 with p-value < 0.01) through Differential Gene Expression (DEG) analysis (Figure2). Two pathways, p53 signaling and IkB-kinase/NFkB signaling, were upregulated in the irradiated group. Consequently, two genes closely associated with these pathways were selected for further investigation, given their high fold-change values (Table2).

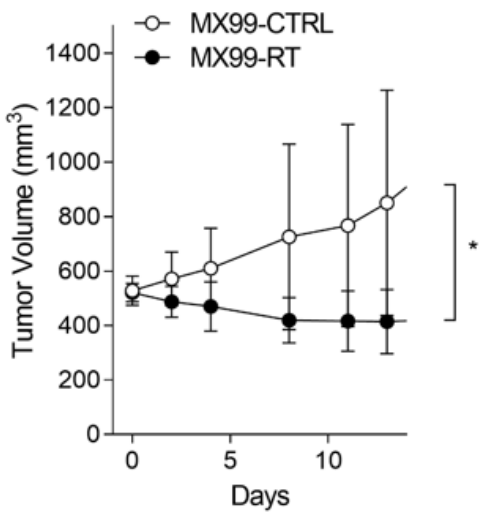


**Figure 1. Tumor growth rate of MX99 patient-derived xenograft (PDX) model with or without irradiation.**

Error bar illustrate mean ± SD. *p≤0.05. p-values were determined by the 2-way ANOVA test.

Table 1. Histopathological Evaluation of Tumor Samples Derived from PDX Models in Control (C) and Irradiated (R) Groups

| | Cellularity | Pleomorphism | Mitosis (/10HPF) | Necrosis | Stromal overgrowth | Mets |
|---|---|---|---|---|---|---|
| C1 | 3 | 2 | 10 | 0 | 0 | 0 |
| C2 | 3 | 2 | 32 | 0 | 0 | 0 |
| C3 | 3 | 2 | 24 | 0 | 0 | 0 |
| R1 | 2 | 1 | 0 | 0 | 0 | 0 |
| R2 | 1 | 1 | 1 | 0 | 1 | 0 |
| R3 | 2 | 2 | 6 | 0 | 1 | 0 |

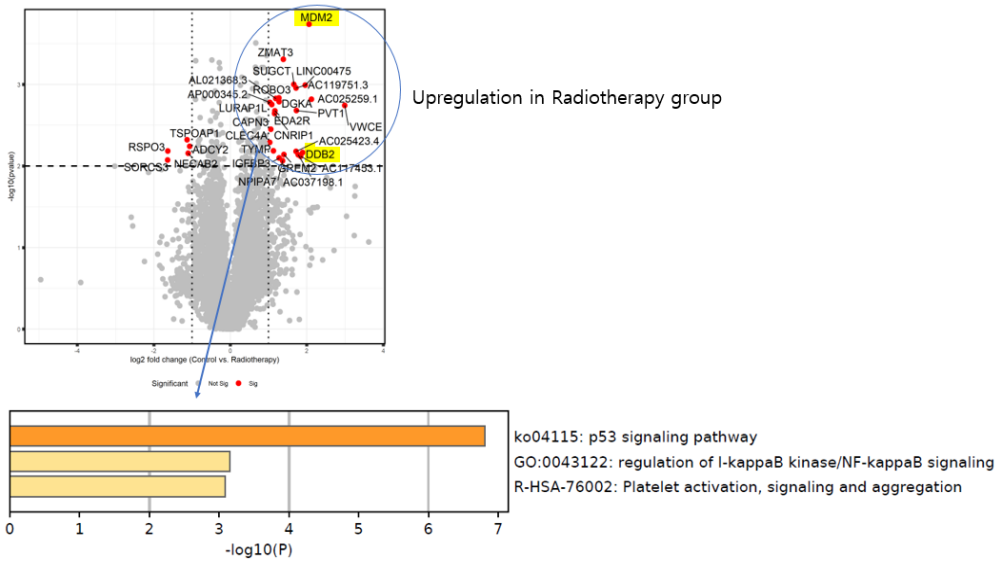


**Figure 2. Identification of key genes potentially associated the radiobiological response of phyllodes tumors.**

Red dots indicate genes that are upregulated in an Irradiation group identified by Differential Gene Expression (DEGs) analysis. KEGG (Kyoto Encyclopedia of Genes and Genomes) pathway analysis identified upregulated signaling pathways in Irradiated group.

**Table 2. Differential Gene Expression Analysis Highlighting the Prominent Upregulation of DDB2 and MDM2 in the Irradiated Group**

| Gene name | P-value | logFC |
|---|---|---|
| MDM2 | 0.000182 | 2.058494 |
| DDB2 | 0.006827 | 1.893563 |

In this study, we focused on the upregulated genes in a radiation therapy group within an in vivo PDX model study, and the subsequent pathways which may contribute to the tumor's response to radiotherapy. One such gene, DDB2 (Damaged DNA Binding Protein 2), is recognized for its involvement in Nucleotide Excision Repair (NER), primarily by participating in DNA binding and UV-related DNA damage recognition, alongside DDB1. This results in high sensitivity to sunlight (xeroderma pigmentosum)

when mutated [6]. It has been suggested that the DDB2-containing complex may also participate in ubiquitin-mediated proteosomal degradation pathways, especially p21 and p53 [7]. Despite these findings, the role of DDB2 in these pathways and its degradation by Cul4A remains debatable [8,9].

On the other hand, MDM2 is a well-documented ubiquitin ligase known as a primary cellular inhibitor of the tumor suppressor protein p53 [10]. MDM2 was also reported to be associated with Retinoblastoma gene product (pRB) ubiquitination and degradation, which can result in pRB downregulation and stimulation of carcinogenesis [11]. MDM2 is often overexpressed or abnormally activated in advanced breast cancer, which suggests its potential oncogenic role [12]. In particular, with addition to our theme, it was suggested that MDM2/X inhibitors along with radiation treatment may help in bringing up the antitumor function of p53, playing a radio sensitizing function [13]. Notwithstanding, some studies indicate a possible opposite function, such as a stabilization role for p53 in a truncated state [14].

In summary, these findings, as well as the demonstrated negative correlation between DDB2 expression levels and histological grade of breast tumors, and the possible tumor-suppressing roles of DDB2 and MDM2, emphasize the necessity for further examination of these genes' roles in malignant phyllodes tumors.

We also used cells derived from the corresponding PDX models to assess the effect of radiation on malignant phyllodes tumors.

# Chapter 2. Materials and Methods

## Cell culture

PDX78 and MX99 cell lines were obtained from patient derived xenograft model through dissociation of tumor cells using tumor dissociation kit for human cells (Miltenyi Biotec., Order no. 130-095-929). All the process was done according to the manufacturing protocol. MDA-MB-231 were purchased from Korean Cell Line Bank in February, 2022. All cell lines were cultured in DMEM high glucose w/stable Glutamine w/Sodium (L0103-500, BIOWEST), supplemented with 10% of fetal bovine serum (FBS) and 1% of penicillin and streptomycin (Solution 100X, L0022-100, BIOWEST). Maintaining conditions are humidified atmosphere with 5% $CO_2$ at 37 ℃.

### siRNA treatment

Pre-designed siRNA targeting human DDB2 (sc-37799) and a scramble control siRNA (sc-37007) were purchased through Santa Cruz Biotechnology (South Korea). Pre-designed siRNA targeting human MDM2 was purchased with Bioneer Corporation (Daejon, South Korea, MDM2-4193-1). Cells were seeded to 6 well plates in an amount of 2.5*10^5 cells/well for MDA-MB-231 and 1.5*10^5 cells/well for PDX78 cells. After 24 hours' siRNA treatment was done in a final amount of 25pmol/well (6 well plates) of needed siRNA using Lipofectamine-RNAiMAX Reagent (13778-150, Invitrogen) and Opti-MEM Medium. Treatment was conducted by the manufacturing protocol. Cells further were incubated for 72 hours at 37 ℃, with media change afterwards before starting sequent experiments, if not said otherwise.

## Radiation treatment

Radiation treatment were conducted using TrueBeam STX. For the preliminary experiments the Radiation dosage ranges in 6, 12, 18, 24, 30 Gy. Due to these preliminary studies further experiments

were later fixated on 24Gy. Media change was performed before applying the radiation and all sequent in vitro analyses were conducted after 24 hours after Radiation applied, if not said otherwise.

## Proliferation Assay

Cells were seeded on flat-bottom 96-well culture plates in a concentration of 3x10^3cells per well for PDX78 cells and 2x10^3cells per well for MDA-MB-231 cells. After their adhesion or after Radiation treatment, cell proliferative count was observed from 0-96 hours. Cells were incubated with 20ul of thiazolyl blue tetrazolium bromide (50ug/ml stock solution, MTT, Sigma-Aldrich) for 2 h at 37° C. The medium was discarded and 200ul of dimethyl sulfoxide (DMSO, Duchefa Biochemie) was added to each well and mixed well with a multipipette to dissolve formazan crystals formed during the incubation. Absorbance was determined at 570 nm using a microplate reader (BioTek Instruments, Vermont, USA). All the data was normalized to the 0 hour values for each sample.

## Apoptosis assay

Apoptosis assay was performed using FITC-AnnexinV Apoptosis Kit (Ref. 556547, BD Bioscience). For FITC-Annexin staining all the processes were performed in a doom light. All cells were included in an analysis, consisting of floating cells in a media and adherent cells, which were detached later by trypsinization. Then, cells were washed with a cold DPBS twice, counted and distributed to the FACS tubes in a concentration of 3-4*10^5 cells / tube. After 5 minutes 1500rpm centrifugation, PBS was discharged and a 1X binding buffer was added in an amount of 100ul. After a gentle vortex PI and Annexin was added to the corresponding tubes (4 tubes for each sample: unstained, PI only, Annexin only, PI and Annexin together). Cells were vortexed gently, incubated for 15 minutes in a room temperature in a dark. 200-300ul of Binding buffer were added to the cell suspension after the incubation and

then cells were analyzed afterwards within 1 hour.

## Migration and Invasion assay analysis

Cells were first harvested by trypsinization and washed with PBS twice. Further, 2*10^5 cells for invasion and 1*10^5 cells for migration analysis, PDX-78 cells were centrifuged and resuspended in 200ul of free media (without FBS). Then this suspension was placed into the 8um pore insert for 24 well usage and full media with FBS was applied outside the insert. For invasion analysis inserts were coated with diluted in free media 1:10 matrigel 30 minutes before ahead under 37C conditions. Cells were incubated for 20 hours and stained afterwards. Fixation contained placing inserts into the methanol for 20 minutes and 10 minutes of paraformaldehyde (PFA) 4% with PBS washing between all stages. Staining was performed with 1% Crystal violet solution, placing inserts in this solution for 2 minutes with further PBS washing and cleaning of the inside part of insert with a wool. After drying up in the air cells were photographed with a bright field in 4X focus.

## Cell Cycle Analysis

For the Cell Cycle Analysis all the process was performed in a doom light. First, adherent cells were detached from the surface by trypsinization. Cells were washed with DPBS twice and resuspended in a small amount of a cold PBS. Further cells were incubated with 5ug/ml of Hoechst 33342 in a dark at a room temperature for 60 minutes and analyzed afterwards. DNA content analysis was carried out in a BD FACS Symphony flow cytometer (BD Bioscience, USA) and analyzed with a FACS software.

## DNA Damage analysis

DNA Damage analysis was performed using a OxiSelect$^{TM}$ Comet Assay Kit (3-well slides) (STA-351, Cell Biolabs). All the incubation periods were performed in a dark, and all the

transporting action should be performed strictly horizontally without disturbing the gel location. After all buffers were prepared and put to the fridge for cooling, agarose was heated for 20 minutes in 95° C and kept at 37° C bath till it needed. After making a base layer of 75ul of agarose on a slide and making it harden in 4° C for 15 minutes, previously prepared cell solution in a cold PBS with a final concentration of 1*10^5 cells were mixed with a warm agarose in a 1:10 ratio. 75ul of this cell suspension in agarose were added above the basal layer and put to 4° C for 15 minutes in the dark. Further incubation of cells in a cold Lysis Buffer was performed for 1 hour at 4° C in the dark conditions, buffer was changed to the Alkaline Solution and incubated for another 30 minutes at 4° C in the dark. Alkaline Solution was then replaced with a pre-chilled TBE Electrophoresis Solution, immersed for 5 minutes and the same process was repeated twice. TBE electrophoresis was performed for 15 minutes at 25 volt conditions. Then glasses were rinsed by immersing it to the pre-chilled distilled water for 2 minutes 3 times, with afterwards replacement for 70% cold Ethanol for 5 minutes. After that slides were let to dry at the dark, then added above with a 100ul/well of diluted 1X Vista Green DNA Dye and incubated for 15 minutes (in the dark), the cell analysis was performed counting about 50-100 cells per sample with a Fluorescent microscopy. Results were analyzed in Tail DNA % calculated by the next formula: Tail length/Cell length*100%.

## Quantitative real time PCR

Total RNA was extracted from cells using Tri-RNA reagent (FATRR001, Favorgen). The reverse transcription of RNA was done by PrimeScript™ RT Master Mix Kit (RR036A, Takara) with a final RNA concentration of 2,5 ug/ul. qPCR assays were conducted using a Power SYBR Green PCR Master mix (Ref.4367659, Thermo Scientific). Reactions were performed on an ABI7500 real-time PCR System (Thermo Scientific, Massachusetts, USA). To analyze the relative mRNA expression levels, all the data was normalized to

the mRNA level of GAPDH and expressed as fold changes against the lowest or the control value. Primers used in this research are illustrated in a Table 3.

Table 3. Sequences of the Primers Used in the Research

Primer sequences used for identification of gene mRNA expression via qPCR technique in human (h) and mouse (m) cells

| Gene | Orientation | Sequence (5'-3') |
|---|---|---|
| h_GAPDH | Forward | GTCTCCTCTGACTTCAACAGCG |
| | Reverse | ACCACCCTGTTGCTGTAGCCAA |
| h_DDB2 | Forward | CCAGTTTTACGCCTCCTCAATGG |
| | Reverse | GGCTACTAGCAGACACATCCAG |
| h_MDM2 | Forward | TGTTTGGCGTGCCAAGCTTCTC |
| | Reverse | CACAGATGTACCTGAGTCCGATG |
| h_p21 | Forward | AGGTGGACCTGGAGACTCTCAG |
| | Reverse | TCCTCTTGGAGAAGATCAGCCG |
| h_p53 | Forward | CCTCAGCATCTTATCCGAGTGG |
| | Reverse | TGGATGGTGGTACAGTCAGAGC |
| m_Gapdh | Forward | CATCACTGCCACCCAGAAGACTG |
| | Reverse | ATGCCAGTGAGCTTCCCGTTCAG |
| m_ddb2 | Forward | GCAAAAGTCGCAGAGGTCCTCA |
| | Reverse | CCTGACAATGCTGCTACTCCGT |
| m_mdm2 | Forward | CCGAGTTTCTCTGTGAAGGAGC |
| | Reverse | GTCTGCTCTCACTCAGCGATGT |

## Western Blotting

To make lysates cells were harvested, washed with DPBS, and frozen at −80℃ before use, then added with RIPA buffer, EDTA 100X and Protease inhibitor Coctail 100X (Ref. 87785, Thermo Fisher). In this state lysates were incubated for 10 min on ice, and centrifuged at 12000 rpm for 15 min at 4° C. Then supernatant was collected and protein concentration was measured. Protein concentration in each sample was analyzed by using Pierce™ BCA Protein assay kit (Ref. 23225, Thermo Scientific). Western Blotting samples were prepared by boiling cell lysates at 95° C for 3 minutes with SDS 5X making an equivalent amount of protein in each sample. Needed amount of protein sample were loaded and separated by sodium dodecyl sulfate−polyacrylamide gel electrophoresis (SDS−PAGE), further transferred to poly−vinylidene fluoride (PVDF; Sigma−Aldrich, missouri, USA) membranes. After the transfer all memranes were checked for transfer efficiency with Ponceau S Staining solution (Ref. A40000279, Thermo Scientific), washed afterwards with a transfer buffer and T−TBS solution consequently. After blocking with 5% Albumin Bovine (BSA, AC1025−100−00, Biosesang) South Korea) T−TBS solution, membranes were incubated with corresponding primary antibodies overnight at 4 ° C. The secondary antibody was diluted (1:5000) in a 5% skim milk T−TBS solution. Protein bands were detected using an Amersham™ Imager 680 (GE Healthcare Life Science, IL, USA) with SuperSignalTM West Pico PLUS Chemiluminiscent Substrate (Ref. 34580, Thermo Scintific) or West Femto Maximum Sensitivity Substrate (Ref. 34095, Thermo Scintific) for weak signals. The following antibodies were used, anti−$\beta$−actin (sc−47778; Santacruz) in 1:2500 dilution, anti−alpha tubulin (A305−798A, Bethyl) with 1:1000 dilution, anti−DDB2 (ab51017, abcam) with 1:700 dilution, anti−MDM2 (SMP14, sc−965, Santacruz technology) with 1:700, dilution, p21 (sc−397, Santacruz technology) with 1:800, dilution, p53 (sc126, Santacruz Technology) with 1:800 dilution, cleaved caspase3 (cst9661, Cell

Signaling Technology) with 1:1000 dilution, cleaved PARP (cst9544, Cell Signaling Technology) with 1:1000 dilution, bcl-2 (sc7382, Santacruz technology) with 1:800 dilution ratio.

## Statistical analysis

GraphPad Prism ver. 9 (GraphPad Software, San Diego, CA, USA) was used to illustrate graphs and perform statistical analysis. Data values are presented as mean ± standard deviation (SD). To analyze the difference between two groups with an element number within 10 values the Mann-Whitney U tests were used. To determine the difference in a Proliferation Assay analysis the 2-way ANOVA was used, as it also includes the time period, as well as 1-way ANOVA to define the difference in a process alone for each sample. P values less than 0,05 were defined as statistically significant.

# Chapter 3. Results and discussion

## Phyllodes tumor cells

The PDX78 and MX99 cells, derived from a patient model, were initially implanted bilaterally into the fat pad region (4th gland). Cell morphologies were established after several passages post-tumor dissociation (Figure 3).

PDX78 cells demonstrated an average proliferation rate of approximately 24-26 hours in DMEM media. Unfortunately, the division speed of MX99 cells could not be determined due to their notably slow growth rate. The size of MX-99 cells ranged from 200 to 300μm, while PDX78 cells measured between 100-300μm. These dimensions are larger than those of typical breast cancer cell lines, such as MDA-MB-231, making them easily observable under 4X magnification.

Interesting observations were made when examining the chromosomal material of phyllodes cells, particularly PDX78, using GTG staining techniques (data not shown). Among all observed metaphase plates of PDX78 cells, most displayed 47 chromosomes with certain abnormalities. However, the detailed interpretation of these abnormalities falls outside our expertise and the scope of this study. Although certain chromosomal abnormalities are known to be associated with different types of phyllodes tumors—for instance, 1q gain and 13q loss in high-grade PTs—identifying such chromosomal alterations could potentially aid in diagnosing tumor type and grade [1].

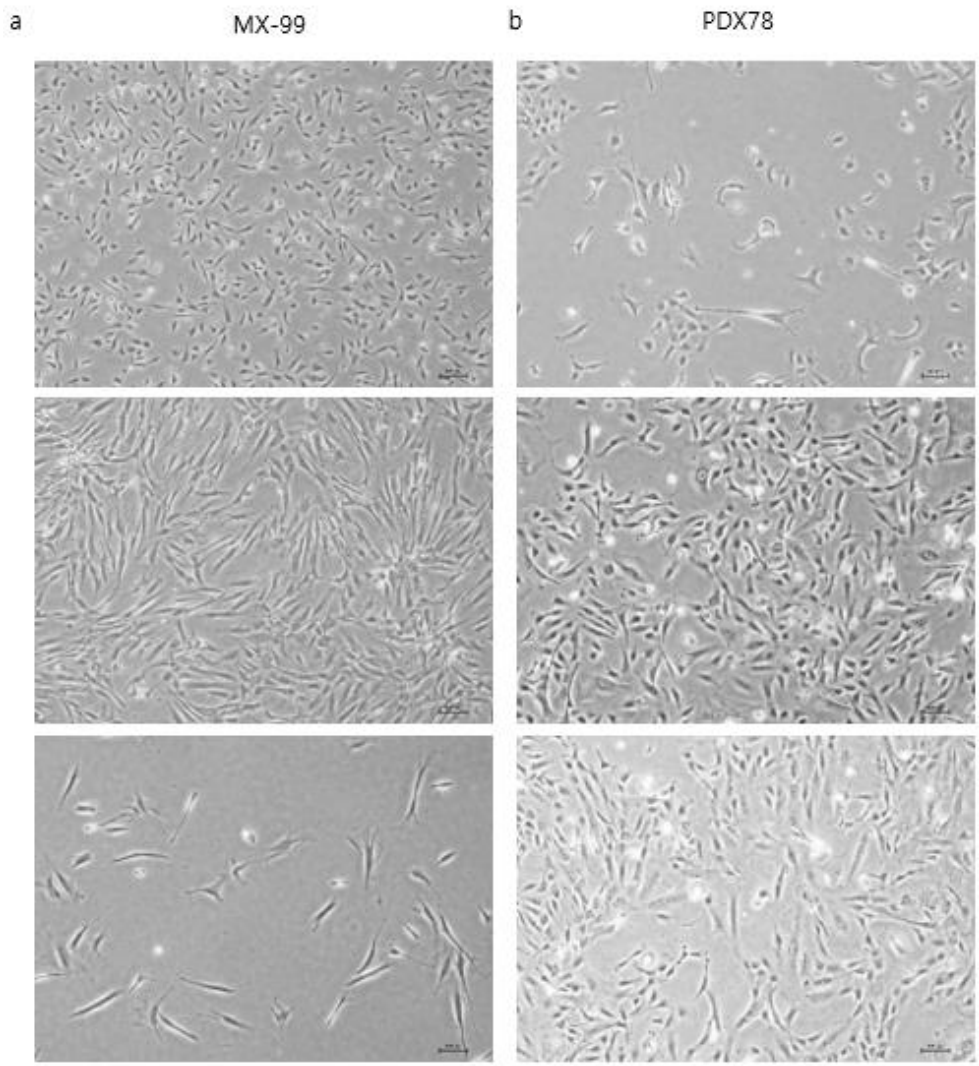


Figure 3. Phyllodes tumor cell lines: cell morphology.

MX99 cell line (a) and PDX78 cell line (b). Illustrated cells are from the passage 0 (after tumor dissociation) in different density (first 2 rows), and after a few passages (last row). All pictures were taken with x4 focus.

## Effects of Radiation on Cell Morphology, Growth Rate, and Expression of Corresponding Genes

Breast cancer cell lines, human and mouse-origin fibroblast cell lines, and phyllodes tumor cells were screened for differential expression of MDM2 and DDB2 genes at the mRNA (using qPCR technique) and protein (using Western Blot) levels (Figure 4). Elevated MDM2 mRNA expression levels were observed in Phyllodes tumor cells and fibroblast-origin cells, whereas DDB2 did not display the same trend. Instead, DDB2 expression increased in non-metastatic cells such as BT474 and MCF7, mirroring results in [15], where it was implicated in breast cancer proliferation and S1/G phase cell cycle progression in non-metastatic cells. The human fibroblast cell line, WI-38, also showed increased DDB2 mRNA expression levels. An elevated level of 60kDa MDM2, believed to play a stabilizing role for p53 [14], was observed at the protein level (Figure 4b).

From this screening, four cell types were selected for further experimentation: PDX78 and MX99 phyllodes tumor cells obtained from primary tumor cells of the PDX mouse model (Figure 1), the MDA-MB-231 TNBC-origin breast cancer cell line, and the human fibroblast cell line WI-38. However, WI-38 was subsequently excluded due to its extremely slow growth rate and the associated challenges this presented for experimental procedures.

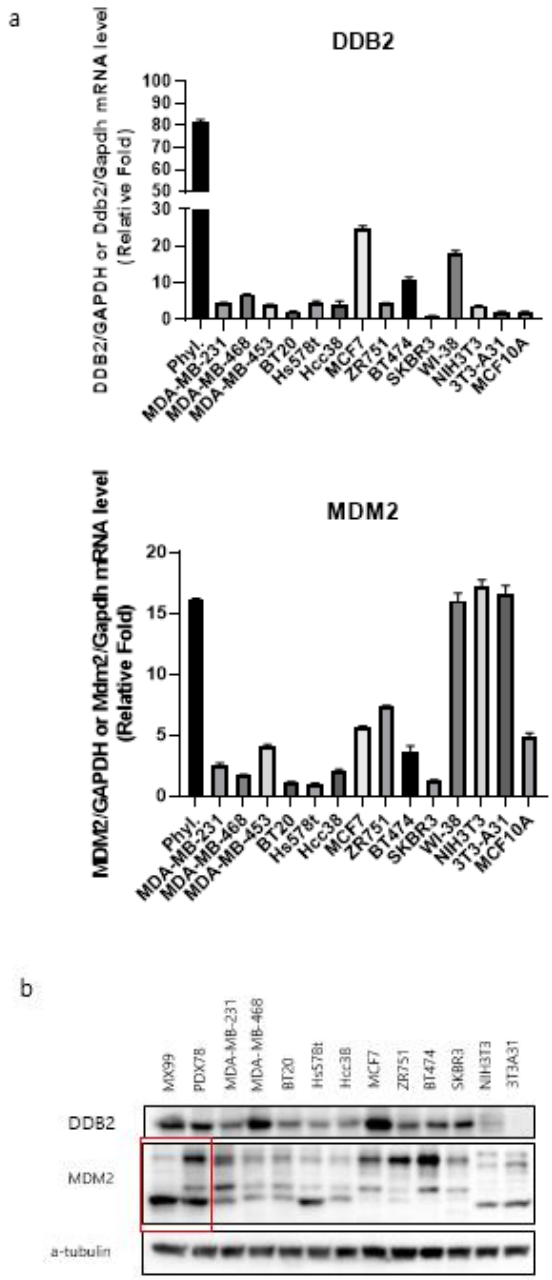


Figure 4. mRNA and protein expression screening of DDB2 and MDM2 gene by qPCR and WB analysis using Breast cancer cell lines, Fibroblast cell lines and Phyllodes Tumor cells.

The relative expression of DDB2 (up row) and MDM2 (below row) were analyzed by qPCR. Data was normalized to the mRNA level of GAPDH and expressed as fold changes against the lowest value. b – Expression of DDB2 and MDM2 measures at the protein

level was determined by Western Blot analysis with b-actin as a loading control.

Similar to the in vivo study, we observed a rapid upregulation of MDM2 (~5.9 fold for 24 Gy) and a modest increase in DDB2 mRNA levels (~1.82 fold for 24 Gy) in RT-treated PDX78 cells (Figure 5a) measured 4 hours post-radiation application. Morphological changes in cells were noticeable after a few passages: radiation-treated cells (6, 12, 18, 24, 30 Gy) appeared more spread out, rounded, and larger in size compared with the untreated control group (Figure 6a). Similar morphological changes were observed for the MDA-MB-231 cell line after 24 Gy radiation treatment, but not for MX-99 cells (Figure 6b). The growth rate of PDX78 cells also decreased in response to radiation, with the most significant changes observed in the 24 and 30 Gy groups (Figure 5b). Unfortunately, growth rate changes in the MX-99 cell line were not observable due to their exceptionally slow proliferation rate, although the cells remained viable.

Taking into account these preliminary findings on gene expression changes following radiation treatment, we determined that the radiation dosage should be fixed at 24 Gy to optimize further experiments, as this dosage also exhibited the most significant difference in MDM2 and DDB2 gene expression between the radiation-treated group and the untreated control (Figure 5a).

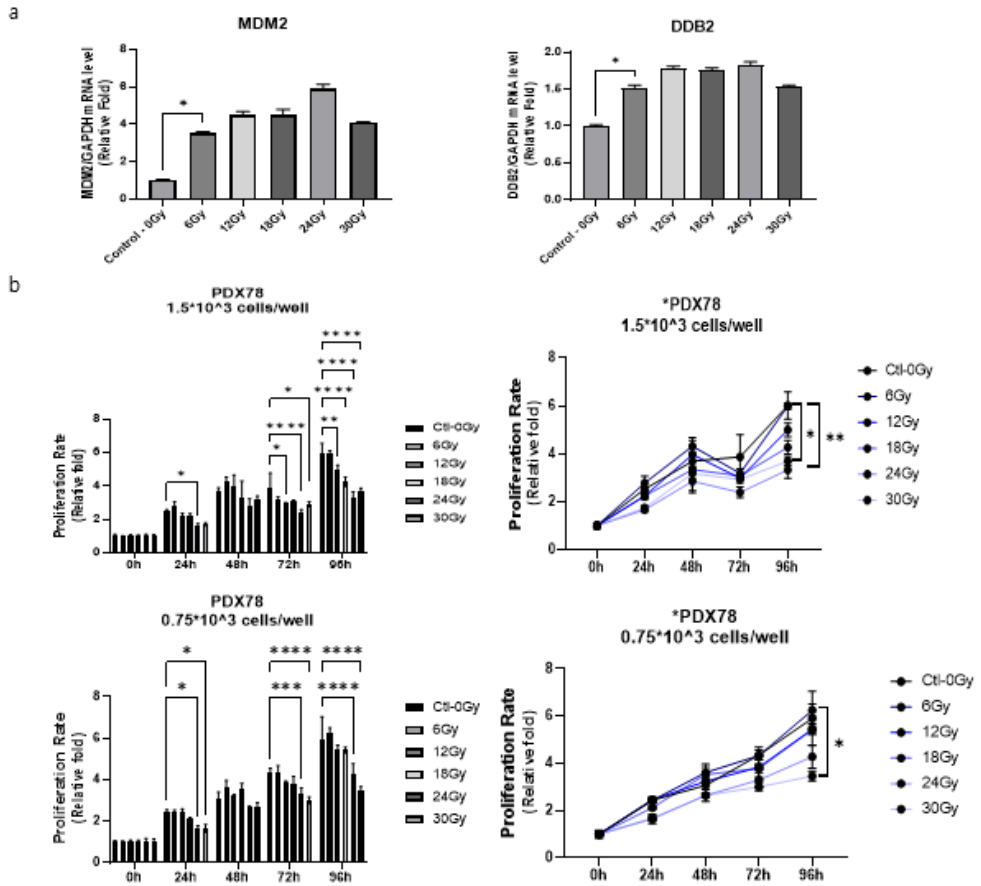


Figure 5. Impact of radiation exposure on the upregulation of targeted genes and the proliferation rate in phyllodes tumor PDX78 cells under in vitro conditions.

a – The relative expression of 2 genes (MDM2 and DDB2) in control and Rt-treated samples (0, 6, 12, 18, 24, 30 Gy) in PDX78 cell line, measured after 4 hours after radiation treatment. qPCR data was normalized to the mRNA level of GAPDH and expressed as fold changes against the control value. Error bars denote mean ± SD. Statistical analysis: non-parametric Mann-Whitney test: *p-value≤0.05 (one-tailed). The statistical difference showed only for the smallest value. b – Growth rate change of PDX78 cells under radiation applied. Growth rate decreases in Rt-treated groups compared with a control sample measured with MTT proliferation assay in different cell concentrations. All data normalised to 0 hour and expressed as a fold change against it. Error bar illustrate mean ± SD. *p≤0.05, **≤0.01, ***≤0.001, ****≤0.0001. p-values were

determined by 2way ANOVA (left) or 1way ANOVA (right) test.

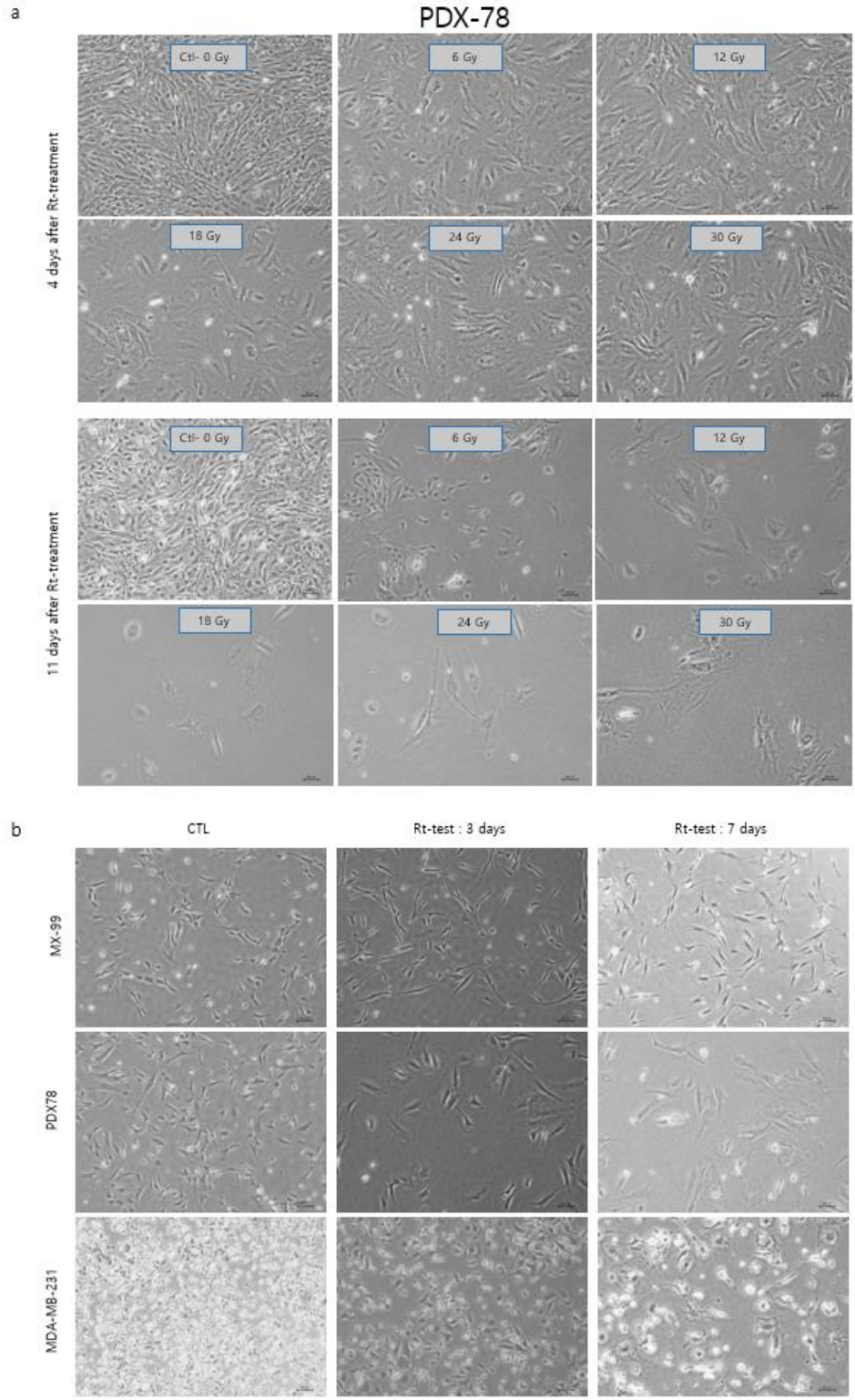


Figure 6. Morphological alterations observed in cells subjected to irradiation.

a – Illustrated PDX78 cells show a different morphology upon radiation applied (6,12,18,24,30 Gy) compared with untreated control sample. It can be seen after 1–2 passages (4–11 days). b – cell morphology change after radiation applied (24Gy) in MX99, PDX78 and MDA–MB–231 cells. All pictures were taken with x4 focus.

To investigate whether the expression of the studied genes is time–dependent post–IR application, we measured mRNA levels using qPCR over timeframes of 4 – 72 hours for MX–99 and 4 hours – 3 weeks for PDX–78 and MDA–MB–231. The shorter timeframe for MX–99 was due to insufficient cell numbers for the experiment. We further confirmed the upregulation of MDM2 and DDB2 in both phyllodes tumor cells, with MX99 cells exhibiting a greater extent of upregulation compared with PDX78 cells. However, upregulation of our genes of interest was only observed in the phyllodes tumor cells (Figure 7 a, b), but not in the breast cancer cell line MDA–MB–231 (Figure 7 c), which was previously considered non–responsive to radiation [16]. MX–99 cells demonstrated a gradual increase in MDM2 and DDB2 mRNA expression levels from 4 to 72 hours post–radiation treatment, while PDX–78 displayed an initial increase followed by stabilization or decrease in mRNA levels within the examined period. Conversely, the MDA–MB–231 cell line showed no stable increase in response to radiation, but rather a constant expression level or even a decrease (Figure 7c). Moreover, these two genes have been proposed as dosimetric for prostate cancer tissue as they were up–regulated even 14 days post a single 10Gy radiation dose and could assist in distinguishing between irradiated and untreated tissues [17]. Given this, DDB2 and MDM2 may play a dosimetric role, but this seems to be specific to certain tissue or cancer types.

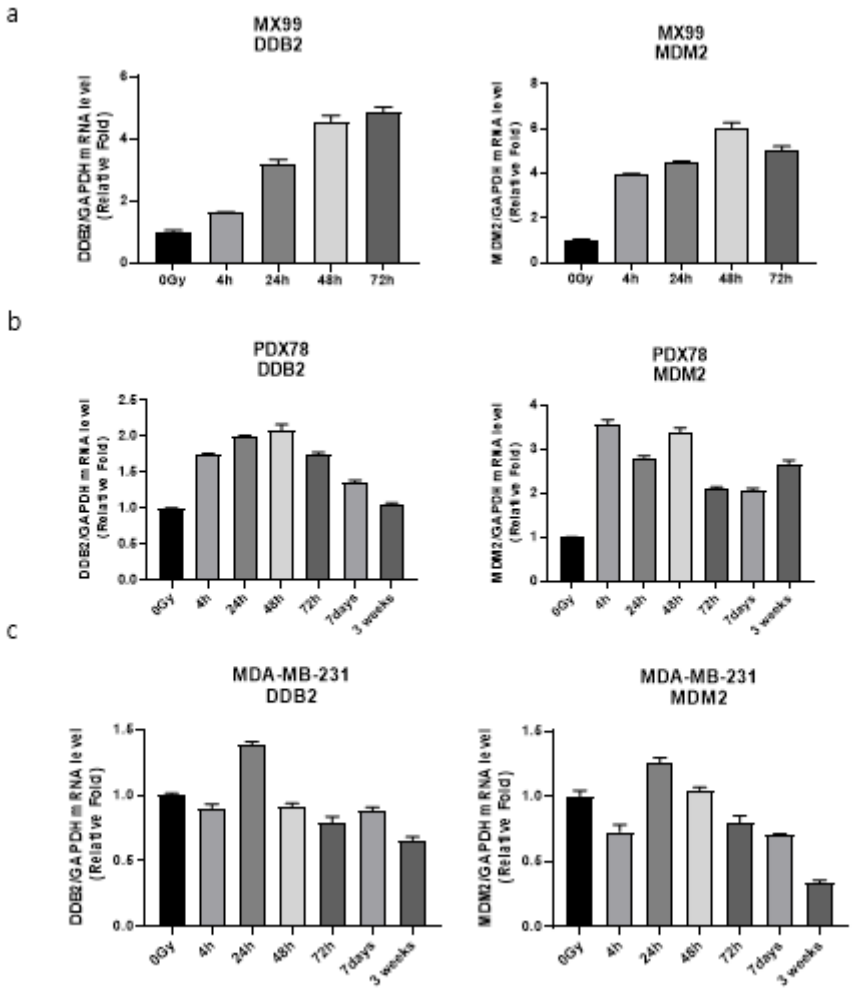


Figure 7. Temporal changes in DDB2 and MDM2 mRNA expression in response to radiation treatment across different cell types.

a – The relative mRNA expression level of DDB2 and MDM2 in Control (0 Gy) and Radiation treated samples (24 Gy) measured after 4h, 24h, 48h, 72h (for MX-99 (a)), 1 week and 3 weeks (for PDX-78 (b) and MDA-MB-231 (c)). All qPCR data was normalized to the mRNA level of GAPDH and expressed as a fold change against the control value. Error bars represent mean ± SD.

## Effect of DDB2 and MDM2 downregulation in PDX78 cells

To understand the impact of the genes of interest on cells, we employed siRNA to silence DDB2 and MDM2 in PDX78 cells. Downregulation of DDB2 resulted in a decreased proliferation rate in PDX78 cells (Figure 8b). This finding aligns with similar results obtained in [15], where an oncogenic role of DDB2 in breast cancer cell lines was identified, increasing cell cycle progression through the G1/S phase. They also reported heightened expression of DDB2 in ER−positive non−invasive cells (MCF7, T47D), but not in ER−negative invasive (MDA−MB−231, SKBR3) breast cancer or normal epithelial cells, corroborating the same results in 16 breast carcinoma patients. This suggests that DDB2 may serve different functions at different stages of breast cancer development. However, contradictory results have been reported for ovarian and prostate cancer [18]. Furthermore, as mentioned earlier, DDB2 was found to play a crucial role in inhibiting migration and invasion processes in aggressive breast cancer, as observed in [19], through upregulation of IkBa and consequent NFkB downregulation. This was further supported by the negative correlation between DDB2 level and histologic SBR grade in the same study of breast carcinoma patients, including 92 samples. Collectively, these findings underscore the duality of DDB2 and cell specificity, highlighting the complexities of studying DDB2.

Radiation treatment appeared to neutralize this effect on the proliferation rate of PDX78 siDDB2 under any radiation dose applied (data shown only for 24Gy), resulting in no significant difference between control and DDB2 downregulated cells (Figure 9b). Figure 8c also shows the proliferation rate of siCTL and siDDB2 treated cells without radiation treatment (first column) and under 6−30Gy radiation (columns 2−6). The associated decrease in proliferation rate for siCTL cells with upregulated DDB2 (Figure 8a) is greater compared to the decrease in the proliferation rate of siDDB2 with a DDB2 downregulated state under radiation. Although the overall

proliferation rate for both siRNA treated cells shows no difference, these results suggest that DDB2 may have separate or distinct functions in cell regulation in upregulated or deficient states, with possible involvement of p21, bcl2 and other regulating molecules [7,19].

Another observable difference in siCTL and siDDB2 radiation-treated PDX78 cells is the increased level of MDM2 in both groups, while DDB2 level only increases in the control group cells (Figure 8a). Cell cycle arrest can occur in DDB2 deficient cells due to the upregulation of p21, but it can only be reached in the presence of MDM2, which defines an independent function of MDM2 from p53 [7]. Hence, we hypothesize a complex network regulating PDX78's reaction under irradiation, involving interconnected signaling pathways for our genes of interest.

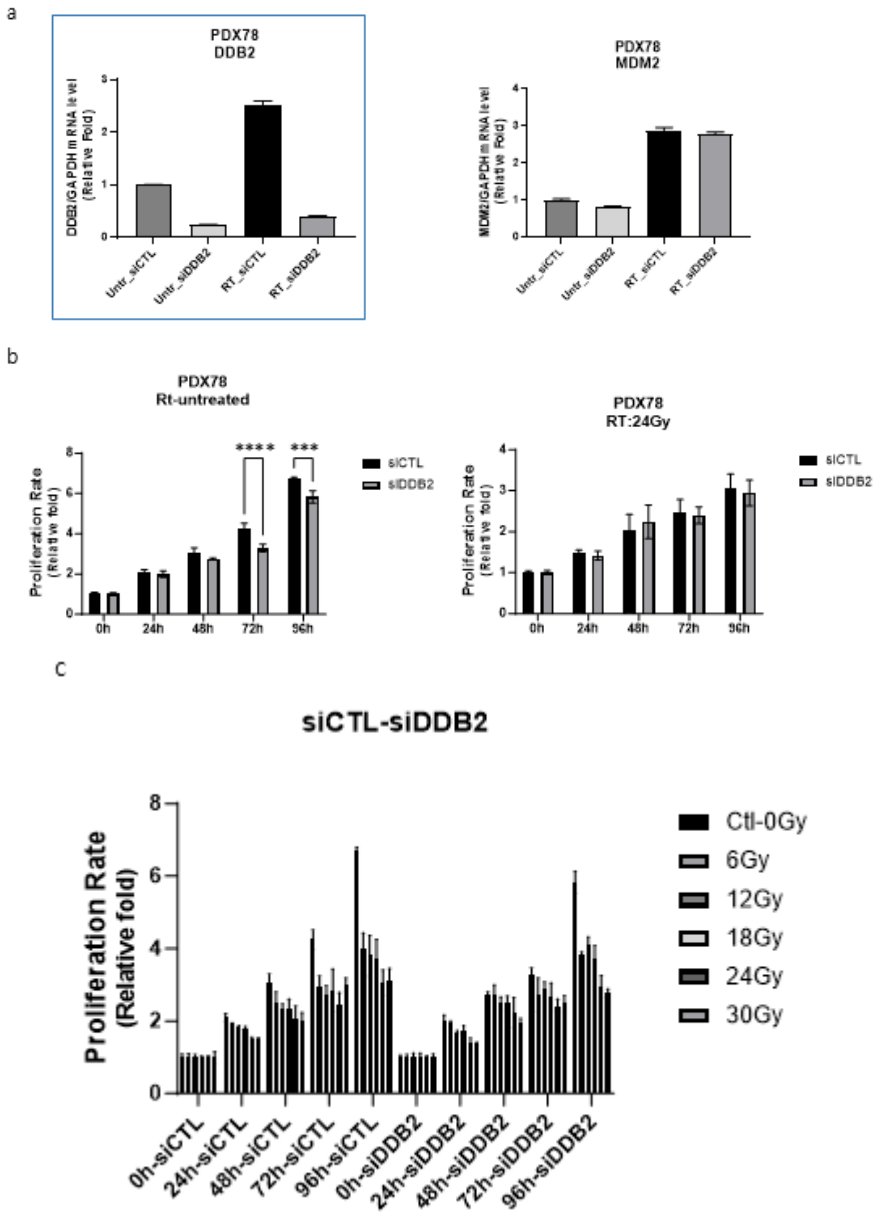


Figure 8. The effect of DDB2 gene silencing on proliferation rate in PDX78 phyllodes tumor cells, and the mitigating impact of irradiation.

a – The relative mRNA expression level of DDB2 and MDM2 measured right after 72 hours' siRNA incubation in PDX-78. All qPCR data was normalized to the mRNA level of GAPDH and expressed as a fold change against the control value. b – Growth

rate change of PDX78 cells with siRNA treatment under 24Gy Rt-treated or untreated conditions. Error bar illustrate mean ± SD. Statistical analysis: 2-way ANOVA. *p≤0.05, **≤0.01, ***≤0.001, ****≤0.0001. c – Growth rate change of PDX78 cells with siRNA treatment under Rt-treated (6-30Gy) or untreated conditions illustrated separately (Statistical analysis is not illustrated due to the complexity of this scheme). All data normalised by 0 hour and expressed as a fold change to it.

Silencing MDM2 resulted in decreased proliferation rate in PDX78 cells (Figure 9b). This decrease in proliferation rate might be due to upregulated p53 activity resulting in cell cycle arrest or apoptosis, considering MDM2's primary function in inhibiting p53, a crucial tumor suppressor, and a significant regulator in a cell.

Radiation treatment resulted in an absence of statistical difference between siCTL and siMDM2 cells, but with the note that this only applies to 24 Gy application. Other dosages maintained decreased values for siMDM2 cells, which is questionable considering the upregulated levels in both siRNA-treated cells.

Also, siMDM2 silencing resulted in a decrease of proliferation itself, and some extra decrease can be seen with radiation applied (with MDM2 upregulation) (Figure 9c), which is opposite with an assumed MDM2 oncogenic role in irradiated conditions [20]. Altogether, according to these results and to two-sided effects of MDM2 reported in [20, 21], we can suggest that MDM2 also may have separate or distinct functions in cell regulation in upregulated or deficient states.

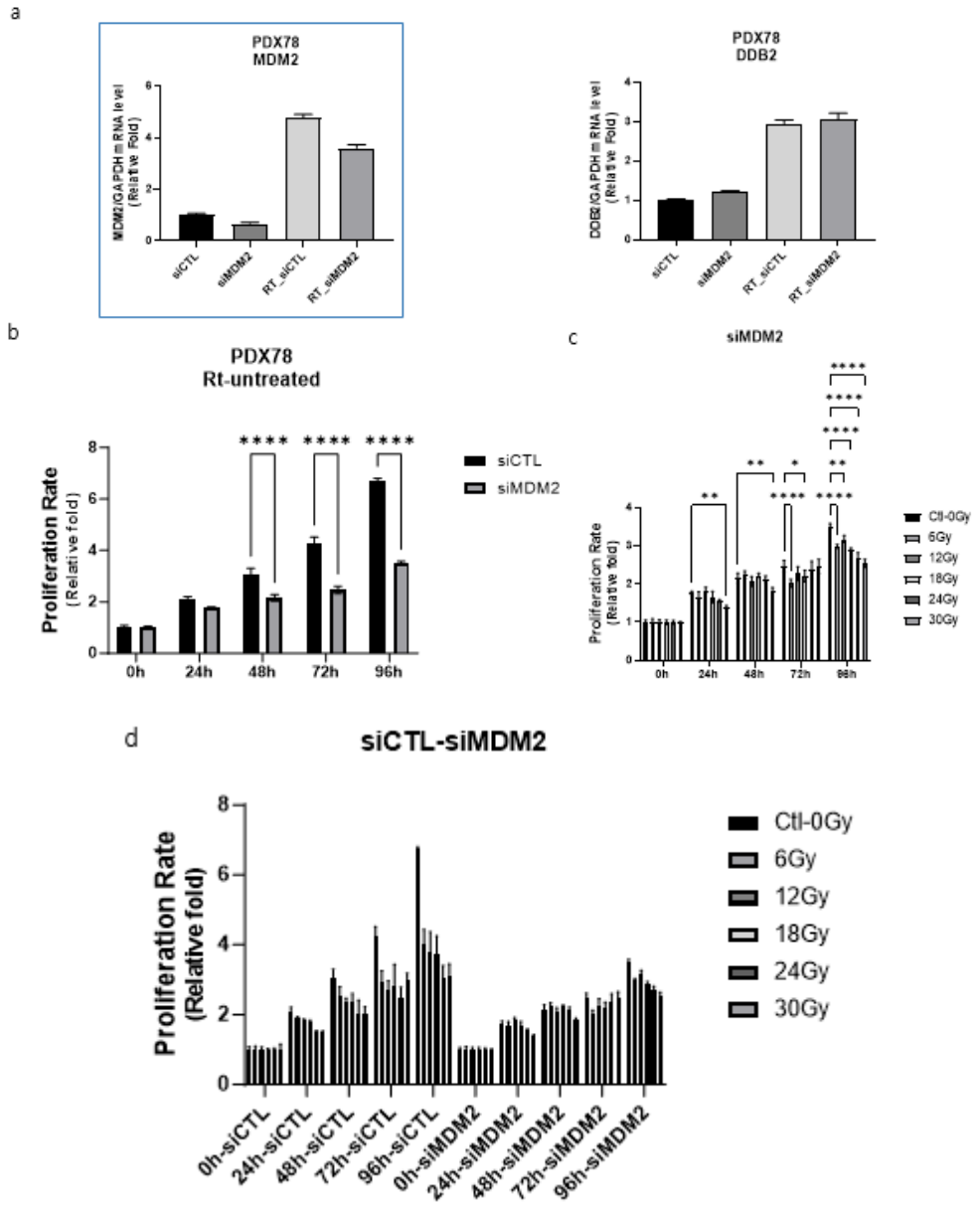


Figure 9. Effects of MDM2 gene silencing on the proliferation rate of PDX78 phyllodes tumor cells, and the augmentation of these effects following radiation-induced MDM2 upregulation.

a - The relative mRNA expression level of DDB2 and MDM2 measured right after 72 hours' siRNA incubation in PDX-78. All qPCR data was normalized to the mRNA level of GAPDH and expressed as a fold change against the control value. b - Growth rate change of PDX78 cells with siRNA treatment under Rt-

untreated conditions. c – Growth rate change of PDX78 cells with siMDM2 treatment under Rt-treated (6-30Gy) or untreated conditions. Statistical analysis: 2-way ANOVA. *p≤0.05, **≤0.01, ***≤0.001, ****≤0.0001. d – Growth rate change of PDX78 cells with siRNA treatment under Rt-treated (6-30Gy) or untreated conditions illustrated separately (Statistical analysis is not illustrated due to the complexity of this scheme). All data normalised by 0 hour and expressed as a fold change to it. Error bar illustrate mean ± SD.

Finally, double siRNA treatment (Figure 10) was conducted based on the assumption that the difference in the proliferation rate between the control and siDDB2 treated group in PDX78 could be due to the upregulation of MDM2 mRNA expression. This preliminary investigation did not yield noticeable differences between siDDB2 treated and siDDB2+siMDM2 treated cells due to the downregulation of MDM2 in DDB2 deficient state. Hence, further investigations need to be conducted. Additionally, while investigating the apoptotic outcome, we observed the upregulation of bcl2 protein under DDB2 deficient state in Figure 10c, supporting involvement of DDB2 in bcl2 [22] and possible apoptosis regulation. In conclusion, the complex nature of DDB2 and MDM2 functions in cell proliferation and the contrasting outcomes with different cancer cell lines indicate the need for further research.

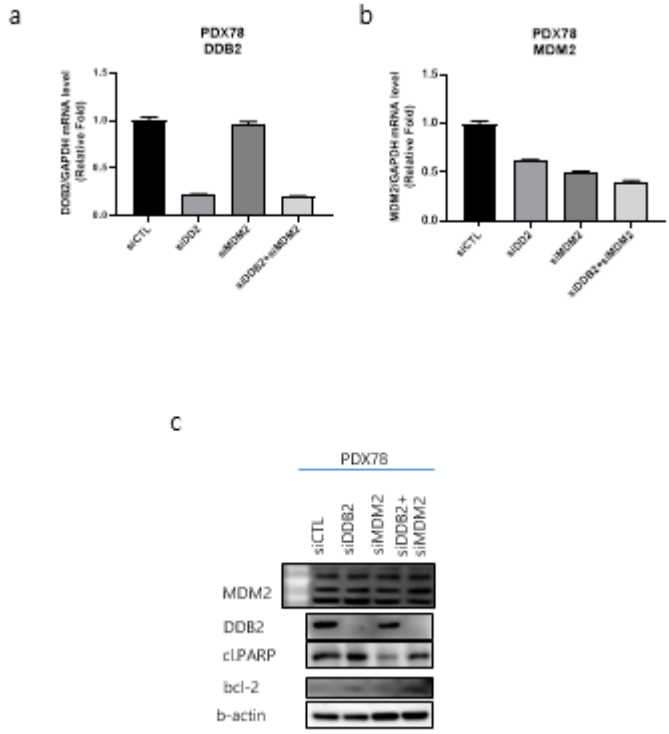


Figure 10. Comparative effects of DDB2 silencing alone and combined DDB2 and MDM2 silencing, with DDB2 downregulation inducing further downregulation of MDM2 expression.

The relative mRNA expression level of DDB2 (a) and MDM2 (b) in PDX-78 cells. All qPCR data was normalized to the mRNA level of GAPDH and expressed as a fold change against the control group value. c - Expression of corresponding genes in the protein level was determined by Western Blot analysis with b-actin as a loading control.

Secondly, we also utilized the Annexin-FITC apoptosis assay in our FACS analysis to discern the differential counts of apoptotic, dead, and live cells. The cells were stained with Annexin-FITC and PI, with the subsequent determination of cell viability based on the selective membrane permeability of these dyes under various states of membrane integrity. Upon confirming the efficacy of siRNA treatment following 72 hours of incubation (Figure 11a), we harvested all cells, including those floating in the medium, for FACS analysis. PDX78 cells displayed an increasing propensity toward apoptosis under conditions of DDB2 deficiency. Combining these results with our proliferation assay findings, we suggest that the observed decrease in growth rate in the DDB2 silenced state could, in part, be attributed to increased apoptosis. These findings are contrary to those in [7], where it was reported that even in a DDB2 deficient state, cells did not undergo apoptosis. Instead, a cell cycle arrest was observed, in opposition to the elevated levels of anti-apoptotic bcl-2. As previously noted, we observed a decreased MDM2 level in DDB2 silenced cells, which is essential for inhibiting apoptosis along with p21.

Conversely, MDM2 silenced PDX78 cells showed a slight increase in apoptotic count, which may also be linked to p53 function. However, overall, we can hypothesize that there is no significant difference between siCTL and siMDM2 cells in apoptotic count.

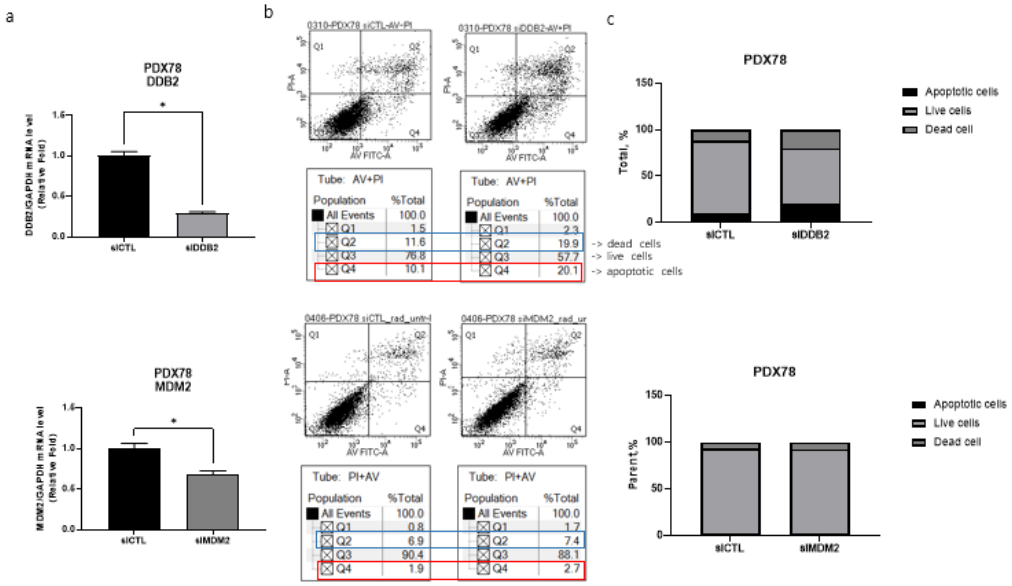


Figure 11. Flow cytometry-based apoptosis assay results for PDX-78 cells following siRNA treatment.

a - The relative mRNA expression level of DDB2 and MDM2 was measured by qPCR in PDX78 cells. All qPCR data was normalized to the mRNA level of GAPDH and expressed as a fold change against the control group value. Error bar illustrate mean ± SD. Statistical analysis: Non-parametric Mann-Whitney test: *p-value≤0.05 (one-tailed). b – representative FACS Annexin V assay results for PDX-78 siDDB2 (upper row) and siMDM2 (below row) treated cells. c – Representative results of total cell count in FACS Annexin analysis for PDX-78 siDDB2 (upper row) and siMDM2 (below row) treated cells.

For PDX78 cells, both untreated and radiation-treated conditions under siCTL exhibited no difference in apoptotic or dead cell count. Nevertheless, with siDDB2 or siMDM2, a slight increase in apoptosis was observed. Intriguingly, the proliferation rate difference between untreated and radiation-treated cells was previously depicted in Figure 5b or 10c. Yet, without a difference in apoptosis for the radiation group, it compels us to explore other mechanisms of cell death or cellular quiescence that we have not accounted for. These findings underscore the complex nature of cellular processes and the variability across different cell lines or cancer types.

Furthermore, we observed that PDX78 cells consistently upregulated DDB2 and MDM2 when subjected to radiation (Figure 12a). This observation lends further support to the proposition that DDB2 and MDM2 could serve as markers for discerning whether tissues or a patient underwent radiotherapy. This was similarly suggested in [17] in the context of prostate cancer patients, albeit with a caveat regarding cell or tissue specificity.

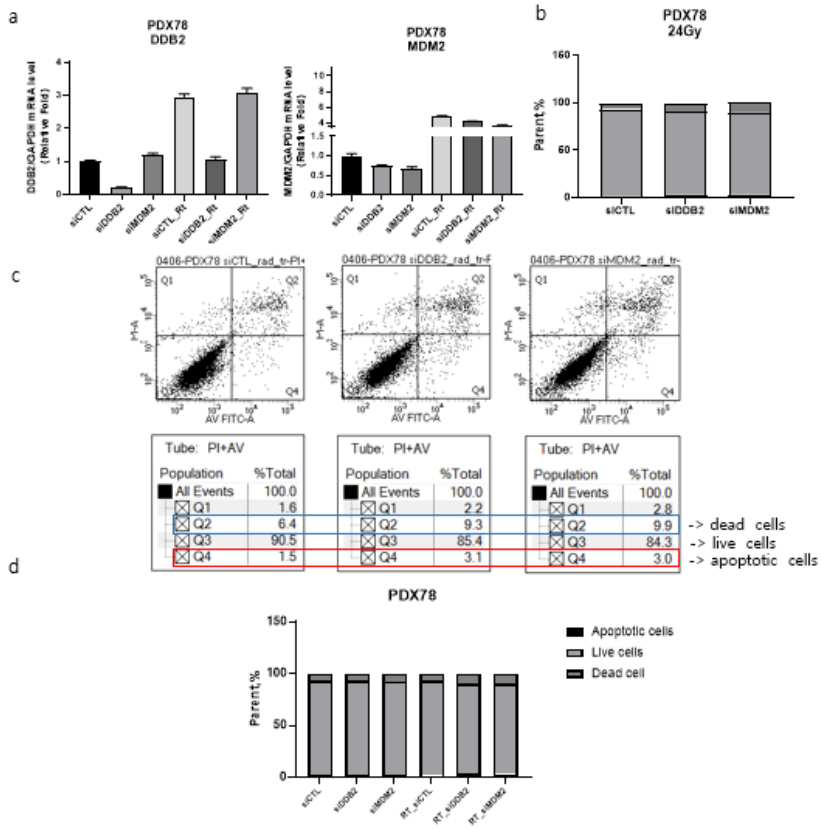


Figure 12. Flow cytometry-based apoptosis assay results for PDX-78 cells subjected to siRNA treatment post-radiation exposure.

a - The relative mRNA expression level of DDB2 and MDM2 was measured by qPCR in PDX78 cells. All qPCR data was normalized to the mRNA level of GAPDH and expressed as a fold change against the control group value. Error bar illustrate mean ± SD. b – Representative results of total cell count in FACS Annexin analysis for PDX-78 siDDB2 and siMDM2 treated cells under 24Gy Radiation applied. c – Representative FACS Annexin V assay results for PDX-78 siDDB2 and siMDM2 treated cells after Radiation applied. d - Representative results of total cell count in FACS Annexin analysis for PDX-78 siDDB2 and siMDM2 treated cells under Rt-untreated or 24Gy Radiation applied conditions.

Given that both genes of interest are involved directly or indirectly in cell cycle progression and apoptosis, it remains challenging to determine their net effect. To confirm the roles of DDB2 and MDM2, we also conducted a cell cycle FACS analysis for PDX78 cells. Regrettably, only adherent cells were utilized for this experiment, excluding the floating cells in the medium. Looking at Figure 13b, we can infer that live DDB2 deficient cells tend toward the S, G2/M transition, with fewer cells in the G0/G1 state. Taken together, we can assert that the proliferative pool of DDB2 deficient cells is greater compared to control cells. Yet, in light of the previous proliferation and apoptosis assay results, it suggests that even though the cells favor the S/G2/M transition, the cell death count is higher, and hence the overall proliferation capacity of DDB2 deficient cells is decreased. These results contradict those presented in [7] and [15]. However, we should consider that PDX78 cells have fibroepithelial origins, as these cells were derived from a phyllodes tumor. These inherent differences may help elucidate the specificity or differences in these cells and their tumorigenic behavior.

In an MDM2 deficient state, PDX78 cells appear to reduce the G2/M phase of the cell cycle without much difference, as seen in Figure 13c. This can be explained by the primary role of MDM2 in inhibiting p53, thus enabling p53 to regulate apoptosis and cell cycle arrest. Additionally, increased apoptosis coupled with a decreased G2/M pool can account for the overall decrease in the proliferation rate of these cells (Figure 9b). We also observed that cells significantly reduced their proliferation rate a few days post-radiation treatment. This led to the cessation of further experiments with cells after an extended period, as the cells usually started to die rapidly and showed considerable cell loss. Thus, the overall observations corroborate the lethal effect of radiation on PDX78 cells.

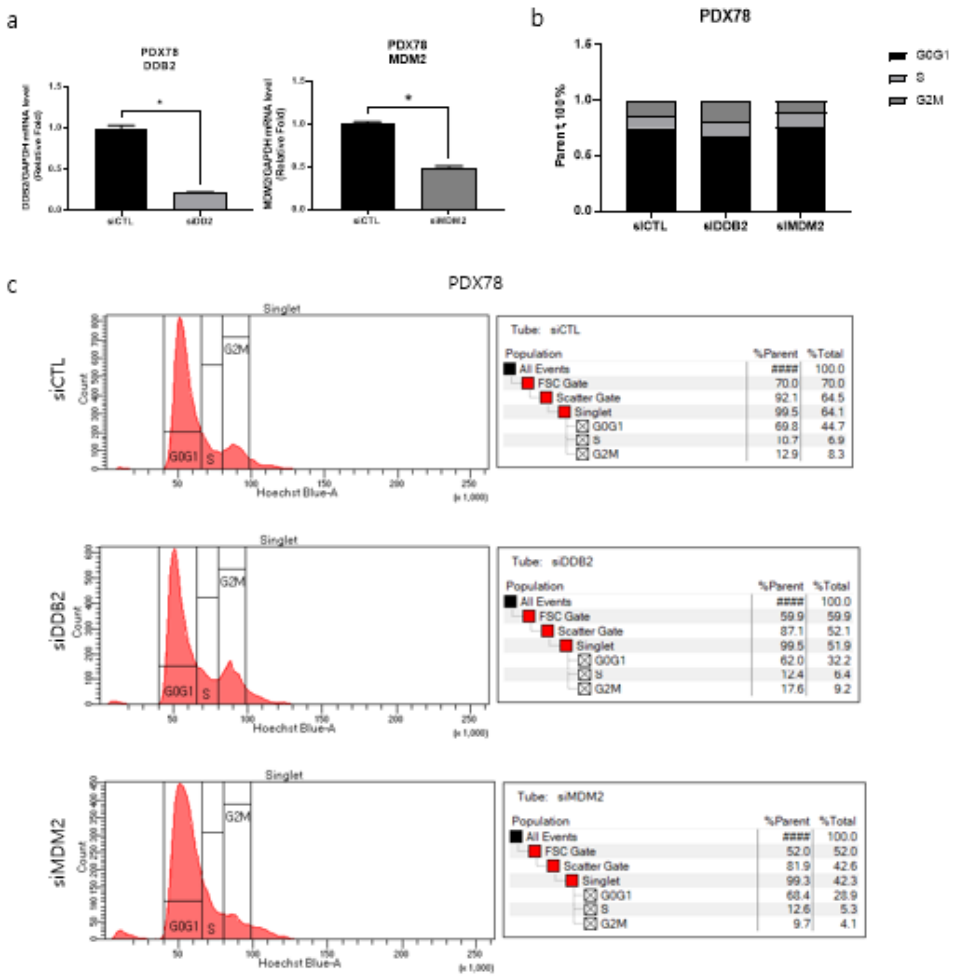


**Figure 13. DDB2 silencing induces S and G2/M phase transition, while MDM2 silencing does not impact cell cycle distribution, as per flow cytometry analyses.**

a – The relative mRNA expression level of DDB2 (left) and MDM2 (right) in PDX78 cells was measured by qPCR. All qPCR data was normalized to the mRNA level of GAPDH and expressed as a fold change against the control group value. Error bar illustrate mean ± SD. Statistical analysis: Non-parametric Mann-Whitney test: *p-value≤0.05 (one-tailed). b – Cell cycle assay results measured by FACS with Hoechst 33342 live staining. c – FACS cell count results for cell cycle DNA content analysis.

As most studies postulate a significant role for DDB2 in regulation pathways related to p53 and p21, and given that p53 is the principal interacting protein with MDM2, we examined the expression levels of p21 and p53 in PDX78 cell lines at both mRNA and protein levels (Figure 14). Upregulation of p53 and p21 in DDB2 silenced PDX78 cells was observed at both mRNA and protein levels under radiation-treated conditions. However, a significant difference in p21 in the non-stimulated state was not observed at the mRNA level, but was apparent at the protein level (Figure 14b-c), supporting the notion of DDB2's role in the proteolytic degradation of p21 [7] and conversely, stabilization of p21 in its absence.

In [23], it was reported that under minor DNA damage, moderate levels of p53 set p21 to assist with cell cycle arrest, allowing DNA repair processes to occur. Conversely, in the same study, they posited a two-stage function of p53 under severe damage. Here, DDB2 plays a role in p21 downregulation, promoting apoptosis with already accumulated pro-apoptotic proteins in the second phase. However, in another radiotherapy study [24], DDB2 was shown to enhance the radioresistance of non-small cell lung cancer (NSCLC) cells through the facilitation of homologous recombination (HR) and the subsequent promotion of double-strand breaks.

Although in [7], the upregulation of p21 was considered to induce cell cycle arrest and inhibit apoptosis in breast cancer cell lines. In our case, p21 failed to inhibit apoptosis, possibly due to the corresponding decrease in MDM2 levels, which was assumed to play a vital role in this. It has also been reported that the complexity of p21 expression changes necessitates careful investigation, considering the distinct functions of each transcript variant. They may respond differently to radiation [25]. Furthermore, p21 itself has been reported to have a dual role in breast cancer, acting as a tumor suppressor in nuclear localization and assisting p53 in cell arrest pathways under DNA damage responses. Conversely, it exhibits oncogenic properties by participating in apoptosis inhibition when localized in the cytoplasm

[26]. Nevertheless, we need to note that the upregulation of p21 was not observed in all experiments but in 60% of PDX78 siDDB2 cells. In other instances, the expression level of p21 was similar between different siRNA-treated cells.

Upregulation of p53 can also be seen even in the non-irradiated state in siDDB2 PDX78 cells. This supports the assumption of DDB2's involvement in p53 proteasomal degradation [9], where upregulated p53, through a positive loop, upregulates the DDB2 protein.

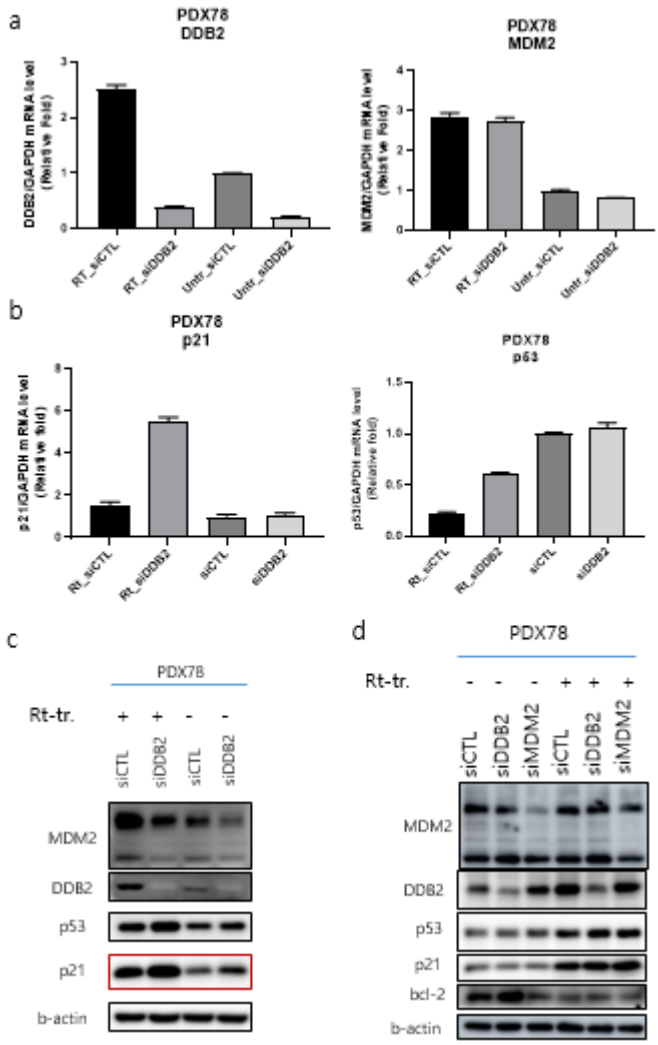


Figure 14. Changes in p21 and p53 expression at mRNA and protein levels associated with DDB2 downregulation, as determined by qPCR and WB analyses.

The relative mRNA expression level of DDB2 and MDM2 (a), p21 and p53 (b) in PDX78 cells was measured by qPCR. All qPCR data was normalized to the mRNA level of GAPDH and expressed as a fold change against the control value. Error bar illustrate mean ± SD. c – Expression of DDB2, MDM2 and related to them proteins, measures at the protein level was determined by Western Blot analysis with b-actin as a loading control.

Additionally, we conducted the migration–invasion assay with PDX78 cells to confirm the previous state about the involvement of DDB2 in migration and invasion processes in Breast Cancer, as their function may still vary in different cancer stages like it was mentioned before. As illustrated in the Figure 15, under the DDB2 or MDM2 deficient state cell migration rate increases in PDX78 cells, suggesting the important role of DDB2 in the migration ability of these cells and actually supporting the assumption that DDB2 plays anti–migration function in some conditions [19], such as aggressive state (PDX78 cells are from the patient with a MPTs). Additionally, DDB2 silencing increasing its migration and invasion capacity can be supported by the negative correlation of DDB2 expression level in SBR grade [19] along with a downregulated state in advanced HNSCC [27], although the role DDB2 in Breast Cancer is considered to be double–sided, as it was shown to also promote the proliferation of nonmetastatic breast cancer cells [15]. In [27] DDB2 was also suggested to be a dominant suppressor of EMT in HNSCC. Same statement was also assumed in [28] for a Colon Cancer.

Also, as it was mentioned in [19] the invasion inhibition maybe associated with an upregulation of IkBa with corresponding inhibition of NF–kB and posterior downregulation of MMP9, which is usually associated with a higher invasive potential of the cells. Overall, along with MnSOD downregulation DDB2 is believed to play an inhibiting role in breast cancer invasion stage [4,19]. Similar results were reported in [29] for a Ovarian Cancer cells describing its involvement in NFkB downregulation and consequent inhibition of tumoregenecity with involvement of transcription factor NANOG.

PDX78 cells also showed nonsignificant but slight increasing invasion capacity in DDB2 deficient state and greater invasion ability in MDM2 deficient state. All together, we can assume, that upregulation of DDB2 and MDM2 in Phyllodes tumor under Radiation applied may play a role in decreasing the migration in invasion capacities of tumor itself, although we failed to check the same data under RT conditions.

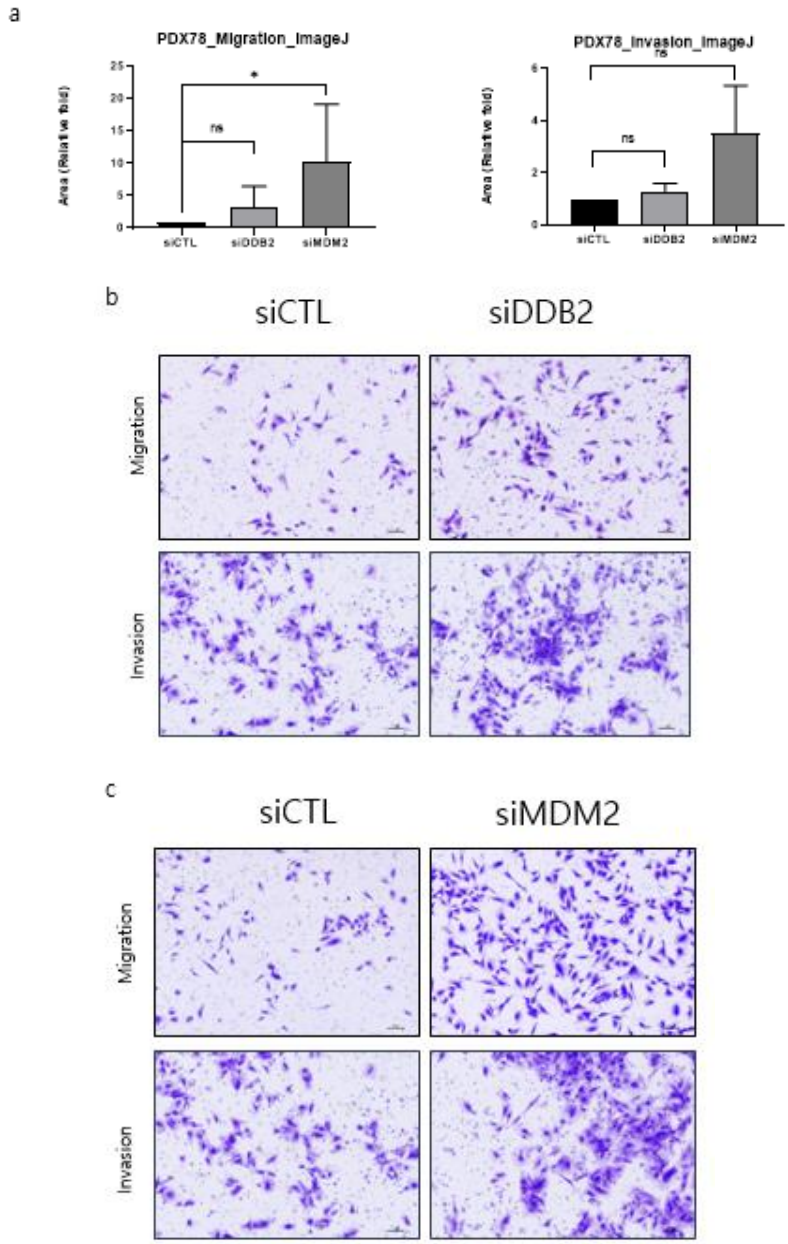


Figure 15. Enhanced migration and invasion capabilities of PDX78 cells resulting from concurrent downregulation of MDM2 and DDB2 genes.

a – Quantitive relative representation of imageJ analysis for migration and invasion assay conducted with PDX-78 cells treated with differenct siRNAs. Error bar illustrate mean ± SD. Statistical analysis: Non-parametric Mann-Whitney test: *p-value

≤0.05 (one-tailed). Representative images of Migration and Invasion assay analysis conducted with PDX-78 cells treated with siDDB2 (b) and siMDM2 (c).

# Conclusions

In this investigation, we observed that malignant phyllodes tumor cells and breast cancer cells exhibit different behaviors and responses to treatment due to their distinct origins. We used an in vivo PDX model study to evaluate the upregulation of genes, specifically DDB2 and MDM2, in response to radiation therapy. Interestingly, we found that upregulation of DDB2 and MDM2 levels is maintained in phyllodes tumor cells and tumor models, but not in breast cancer cells. This upregulation was evident as soon as 4 hours after radiation and persisted for up to 3 weeks.

We observed that cells deficient in DDB2 and MDM2, both exhibited a decreased proliferation rate. Interestingly, the effect of radiation treatment nullified the difference in proliferation rate seen before, suggesting that other genes may be upregulated in response to radiation. However, DDB2 deficiency seems to drive the S/G2M transition in the cell cycle, even though apoptosis generally overrides this effect.

On the other hand, MDM2 deficiency did not significantly affect apoptosis or cell cycle distribution. Intriguingly, cells treated with siDDB2 showed a slight increase in apoptosis, contradicting previous studies. This might be due to an increase in p21, a key player in cell cycle arrest and apoptosis inhibition, which fails to inhibit apoptosis due to the corresponding decrease in MDM2 level.

Moreover, silencing of DDB2 and MDM2 has a tendency to increase the invasion ability of PDX78 cells. This suggests that upregulation of DDB2 and MDM2 under radiation might contribute to the reduction of tumor cell migration and invasion capacities. However, further investigations under radiation conditions are required to validate this hypothesis.

Taking into account the complexity of the cells studied, the interconnectedness of the MDM2 and DDB2 pathways, and the difficulties with radiation-treated cell counts, it was challenging to draw a definitive conclusion about the effect of radiation on the cells investigated. For future studies, an individual approach to each cell

line used in the research should be considered.

Notably, our in vivo studies indicate a potential positive role for the upregulation of DDB2 and MDM2 genes in PDX78 cells, including an increase in cell cycle arrest. We also propose that upregulation of these genes may contribute to the suppression of tumor invasion and migration abilities, based on corresponding in vitro analysis.

Despite these findings, it is imperative to further investigate the complexity of DDB2 and MDM2 networks, considering their varied effects in deficient or upregulated states. The use of overexpressed cells might be helpful in drawing further conclusions on the role of DDB2 and MDM2 in the responses of phyllodes tumor cells to radiation. However, conducting this under our conditions was impossible, considering the already high expression levels of these genes in the cells we used.

# References


1. Zhang Y., Kleer C.G. Phyllodes Tumor of the Breast Histopathologic Features, Differential Diagnosis, and Molecular/Genetic Updates / Y. Zhang, C.G. Kleer // Arch Pathol Lab Med. – 2–16. – Vol 140. – p. 665–671.
2. Fede, A.B.d.S. Malignant Phyllodes Tumor of the Breast: A Practice Review / A.B.d.S. Fede [et al.] // Clin. Pract. – 2021. – Vol. 11. – p. 205–215.
3. Cheo F.F. An update on the classification of phyllodes tumours of the breast / F.F. Cheo [et al.] // Diagnostic histopathology. – 2021. – Vol. 28 (3).
4. Minig V. Identification of DDB2 Protein as a Transcriptional Regulator of Constitutive SOD2 Gene Expression in Human Breast Cancer Cells / V. Minig [et al.] // The journal of biological chemistry 2009. – Vol. 284 (21). – p. 14165–14176
5. Lissidini G. Malignant phyllodes tumor of the breast: a systematic review / G. Lissidini [et al.] // Patologica. – 2022. – Vol.114. – p.111–120.
6. Tang J., Chu G. Xeroderma pigmentosum complementation group E and UV damaged DNA–binding protein / J. Tang, G. Chu // DNA Repair (Amst). – 2002. – Vol 1 (8). – p. 601–616.
7. Stoyanova T.  DDB2 decides cell fate following DNA damage / T. Stoyanova [et al.] // PNAS. – 2009. – Vol. 106 (26). – p. 10690–10695.
8. Stoyanova T. DDB2 (Damaged DNA binding protein 2) in nucleotide excision repair and DNA damage response / T. Stoyanova [et al.] // Cell Cycle. – 2009. – Vol. 8(24). – p. 4067–4071.
9. Tan T., Chu G. p53 Binds and Activates the Xeroderma Pigmentosum DDB2 Gene in Humans but Not Mice / T. Tan, G. Chu // Molecular and Cellular Biology. – 2002. – Vol. 22 (10). – p. 3247–3254
10. Wang S. Targeting the MDM2–p53 Protein–Protein

Interaction for New Cancer Therapy: Progress and challenges / S. Wang [et al.] // CSH Prespectives in Medicine. – 2017. – Vol. 7.
11. Uchida C. Enchanced MDM2 activity inhibits pRB function via ubiquitin-dependent degradation / Uchida C. [et al.] // The EMBO Journal. – 2005. – Vol. 24. – p. 160-169.
12. Qin J.J. Experimental Therapy of Advanced Breast Cancer: Targeting NFAT1-MDM2-p53 pathways / J.J. Gin [et. al] // Prog.Mol.Biol.Transl.Sci. – 2019. – Vol. 151. – p. 195-216.
13. Miles X., MDM2/X Inhibitor as Radiosensitizers for Glioblastoma Targeted Therapy / X. Miles // Front. Oncol. – 2021. Vol. 11.
14. Oliver T.G. Caspase-2-mediated cleavage of MDM2 created a p53-induced positive feedback loop / T.G. Oliver. [et al.] // Molecular Cell. – 2011. – Vol.43 (1). – p. 57-71.
15. Kattan Z. Damaged DNA Binding Protein 2 Plays a Role in Breast Cacner Cell Growth / Z. Kattan [et al.] // PLoS ONE. – 2008. – Vol. 3 (4).
16. Lautenschlaeger T. In vitro study of combined cilengitide and radiation treatment in breast cancer cell lines / T. Lautenschlaeger [et. al] // Rasiation Oncology. – 2013. – Vol. 8.
17. Keam S.P. Biodosimetric transcriptional and proteomic changes are conserved in irradiated human tissue / S.P. Keam [et al.] // Radiation and Environmental Biophysics. – 2018. – Vol. 57. – p. 241-249.
18. Gilson P. Emerging roles of DDB2 in cancer / P. Gilson [et al.] // International Journal of Molecular Sciences. – 2019. – Vol. 20.
19. Ennen M. DDB2: A Novel Regulator of NF-kB and Breast Tumor Invasion / M. Ennen [et al.] // Cancer Res. - 2013. - Vol. 73 (16).
20. Perry M.E. MDM2 in the response to radiation / M.E. Perry // Mol Cancer Res. – 2004. – Vol 2(1). – p. 9-19
21. Cao Z. MDM2 promotes genome instability by ubiquitinating the transcription factor HBP1 / Z. Cao [et. al] // Oncogene. – 2019. – Vol. 38 (24). – p. 4835-4855.

22. Zhao R. DNA Damage-Binding Complex Recruits HDAC1 to Repress Bcl-2 Transcription in Human Ovarian Cancer Cells / Zhao R. [et. al] // Mol. Cancer Research. – 2014. – Vol. 12 (3). – p. 370-380.
23. Li H. Coordination between p21 and DDB2 in the Cellular Response to UV Radiation / H. Li [et. al.] // PLoS One. – 2013. – Vol. 8 (11).
24. Zou N. DDB2 increases radioresistance of NSCLC cells by enhancing DNA damage responses / N. Zoe [et. al] // Tumor Biol. – 2016. – Vol. 37 (10). – p. 14183-14191
25. Danyaei E. Effect of Ionizing Radiation on the Transcript Variants Expression of p21 Gene / E. Danyaei [et. al] // Asian Pac. J. Cacner Prev. – 2021. – Vol. 22 (11). – p. 3717-3722.
26. Zohny S.F. $p21^{Waf/Cip1}$: its paradoxical effect in the regulation of breast cancer / Z.F. Zohny [et. al] // Breast Cancer. – 2019. – Vol. 26. – p. 131-137.
27. Bommi P.V. DDB2 regulates Epithelial-to-Mesenhymal Transitiom (EMT) in Oral/Head and Neck Squamous Cell Carcinoma / P.V. Bommi [et. al] // Oncotarget. – 2018. – Vol. 9 (78). – p. 34708-34718.
28. Roy N. DDB2 suppresses epithetial-to-mesenchymal transition in colon cancer / N. Roy [et. al] / Camcer Res. – 2013. – Vol. 73 (12). – p. 3771-82
29. Han C.H. DDB2 Suppresses Tumorigenicity by Limitting the Cancer Stem Cell Population in Ovarian Cancer / C.H. Han [et. al] // Mol. Cancer Research. – 2014. – Vol. 12 (5). – p. 784-794.

# Abstract

유방 악성종양의 일차 치료는 수술적 절제술이며, 효과적인 전신치료법이 없다. 수술절제연을 확보하여 수술을 시행해도 국소재발률이 높기 때문에 이를 낮추기 위한 노력으로 보조 방사선 요법을 시행하기도 하나, 그 역할은 명확하지 않다. 본 연구에서 유방 악성엽상종양 이종이식모델을 이용하여 방사서 치료의 영향을 분석하였다. 방사선 치료를 받은 그룹이 대조군에 비해 종양의 성장 억제가 유의하게 있었고, 유사 분열 수가 감소하였다. 또한, 조직학적 분석에서 방사선 치료군에서 Stromal cellularity와 Pleomorphism의 경향이 감소하는 것을 나타냈다. 절제한 종양조직을 이용하여 시행한 유전자 발현(DGEs) 분석에서는 p53 신호 경로와 I-kappa B kinase/NF-kappa B 신호 경로의 상향 조절이 발견되었다. 이러한 경로와 관련된 두 가지 유전자, MDM2와 DDB2가 방사선을 받은 그룹에서 상당히 상향 조절(upregulation)되었다. 우리는 방사선이 유도한 DDB2와 MDM2의 상향 조절이 악성엽상종양 세포와 종양 모델에서 보존되지만, 유방암 세포에서는 그렇지 않다는 것을 발견하였다. 또한, DDB2와 MDM2가 저발현된 세포들은 증식 속도가 감소하였다. DDB2 저발현은 S/G2M 세포주기 전환을 촉진하는 경향이 있지만, 본 실험에서는 세포사멸 (apoptosis)이 더 우세하게 나타났다. 본 연구에서 DDB2와 MDM2의 상향 조절이 유방 악성종양세포에서 방사선 내성에 기여한다는 증거를 찾지못했다. 그러나, 우리는 이들 유전자의 상향 조절이 방사선 치료의 효과 하에 유방 악성종양 세포의 증식을 감소시키는 역할을 할 수 있다고 추정할 수 있다.

**Keywords:** Phyllodes tumor, Radiation therapy, PDX model, DDB2, MDM2
**Student Number:** 2021-22873

본 논문작성자는 한국정부초청장학금(Global Korea Scholarship)을 지원받은 장학생임